

Supporting Material for:

Inquiry of the Electron Density Transfers in
Chemical Reactions. Complete Reaction path
for the Denitrogenation Process of 2,3
diazabicyclo[2.2.1]hept-2-ene Derivatives

Vicent S. Safont,¹ Patricio González-Navarrete,^{1,2} Mónica Oliva¹ and Juan Andrés¹

¹Departamento de Química Física y Analítica, Universitat Jaume I, Avda. Sos Baynat
s/n, 12071, Castelló de la Plana, Spain.

² Author present address: Institut für Chemie, Technische Universität Berlin Straße des
17 Juni 135, 10623 Berlin, Germany

E-mail: andres@qfa.uji.es

Table 1S. Relative (to DBH in its closed-shell singlet state) energies (kcal/mol) of the stationary points found. Total energies (hartrees/particle) of DBH reactant are also reported. Energies of open-shell singlet species do not include spin projection corrections.

	B3LYP/ 6-31G(d)	B3LYP/ 6-311+G(2d,p)	M05-2X/ 6-31G(d)	M05-2X/ 6-311+G(2d,p)
DBH total energy	-304.793475	-304.880853	-304.757124	-304.844921
<i>Migration pathway</i>				
TSm-DBH	49.74	42.87	57.40	52.09
CP-DBH + N ₂	-36.27	-43.53	-31.81	-37.72
<i>Concerted open-shell singlet-state pathway</i>				
TSc-DBH	40.48	37.11	46.87	44.10
DBH-diyl + N ₂	25.39	18.29	32.52	26.77
BCP-DBH + N ₂	-6.83	-12.20	-4.13	-8.18

Table 2S. Relative (to DBOH in its closed-shell singlet state) energies (kcal/mol) of the stationary points found. Total energies (hartrees/particle) of DBOH reactant are also reported. Energies of open-shell singlet species do not include spin projection corrections.

	B3LYP/ 6-31G(d)	B3LYP/ 6-311+G(2d,p)	M05-2X/ 6-31G(d)	M05-2X/ 6-311+G(2d,p)
DBOH total energy	-455.220662	-455.375167	-455.176952	-455.332228
<i>Migration pathway</i>				
TSm-DBOH	66.03	61.95	75.52	71.75
CP-DBOH + N ₂	-37.38	-45.23	-31.06	-37.59
<i>Stepwise open-shell singlet-state pathway</i>				
TSS1-DBOH	37.53*	35.03	41.78*	39.73
I-DBOH	36.11	33.31	41.55	39.34
TSS2-DBOH	37.86	34.21	44.64	41.68
DBOH-diyl + N ₂	20.86	12.23	29.44	22.50
BCP-DBOH	-7.92	-13.52	-4.14	-8.29

* These stationary points could not be fully optimized at the theoretical level indicated, and the reported energies have been calculated at the B3LYP/6-31G(d)//B3LYP/6-311+G(2d,p) or M05-2X/6-31G(d)//M05-2X/6-311+G(2d,p) levels.

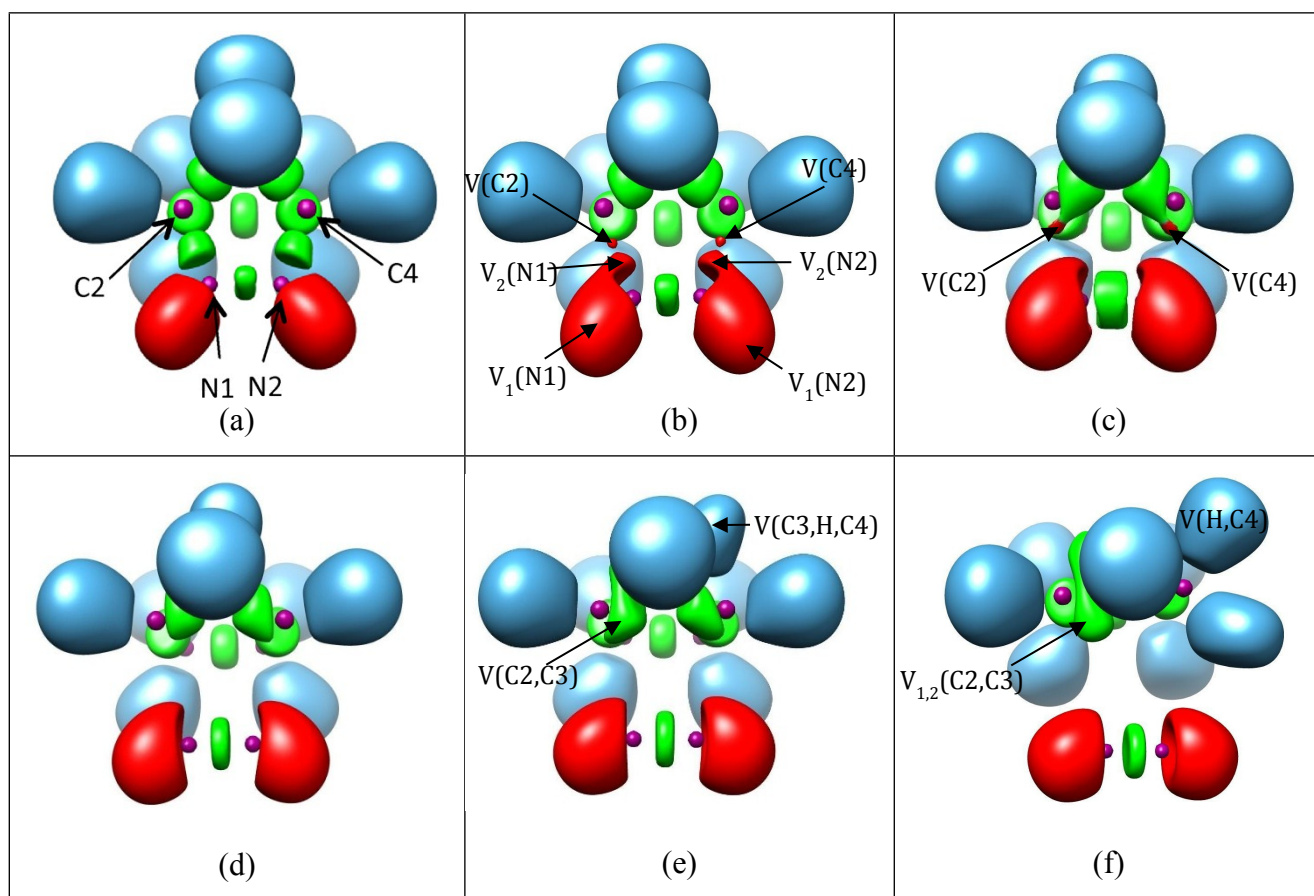


Figure 1S. Snapshots of the ELF localization domains ($\eta = 0.8$ isosurface except where indicated) for selected points along the IRC of the denitrogenation of DBH via *migration* reaction pathway: (a) DBH belonging to SSD-I, (b) point at $s = -4.60 \text{ amu}^{1/2} \text{ bohr}$ ($\eta = 0.785$ isosurface) belonging to SSD-II, (c) point at $s = -2.30 \text{ amu}^{1/2} \text{ bohr}$ ($\eta = 0.731$ isosurface) belonging to SSD-III, (d) TSm-DBH belonging to SSD-IV, (e) point at $s = 1.69 \text{ amu}^{1/2} \text{ bohr}$ belonging to SSD-V, (f) CP-DBH plus N₂, belonging to SSD-VI. The color code is as follows: green, disynaptic basins; red, monosynaptic basins; blue, hydrogenated basins; purple, core basins.

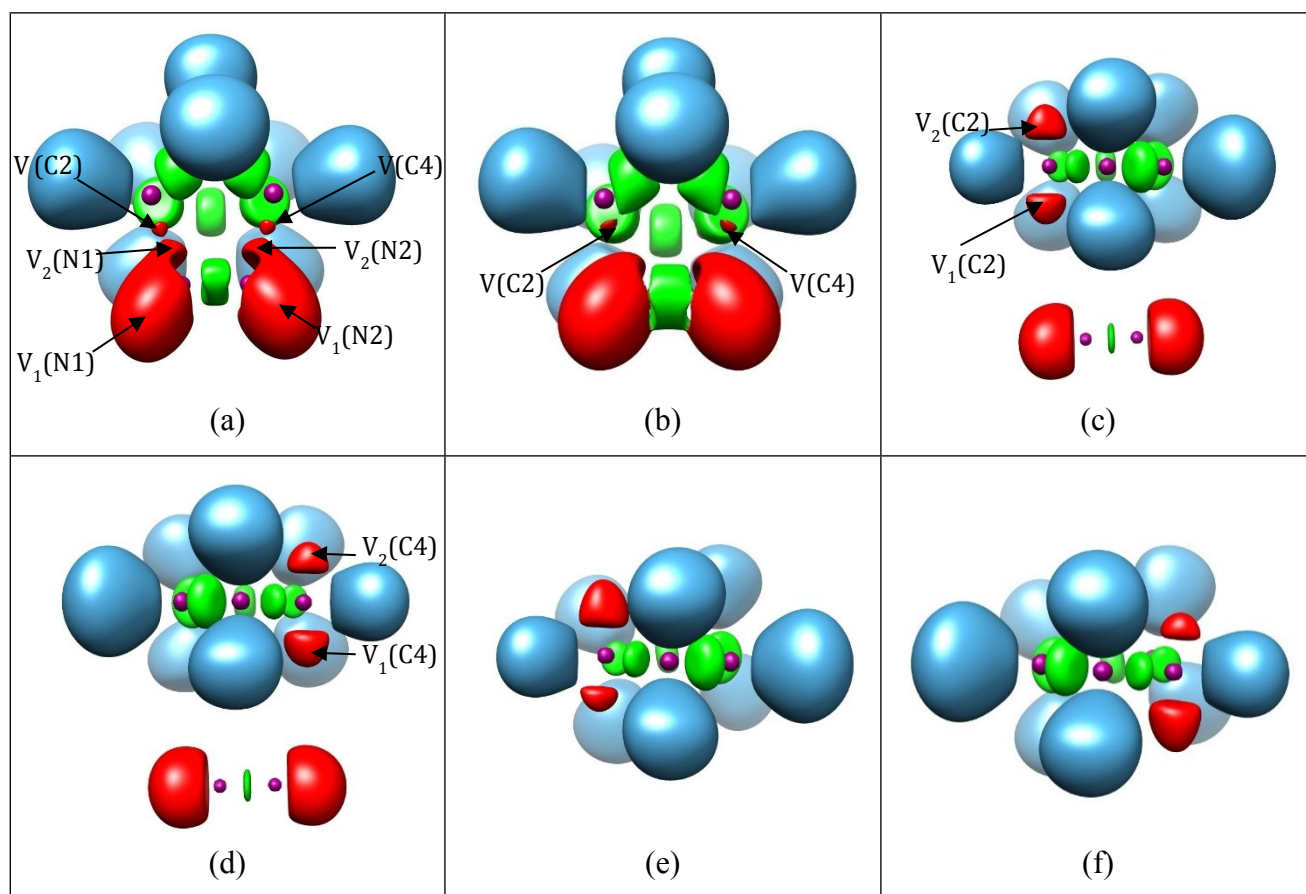


Figure 2S. Snapshots of the ELF localization domains for selected points along the IRC of the denitrogenation of DBH via *concerted* reaction pathway (see DBH belonging to SSD-I in Figure 1Sa): (a) point at $s = -1.68 \text{ amu}^{1/2} \text{ bohr}$ ($\eta = 0.755$ isosurface) belonging to SSD-II, (b) TSc-DBH ($\eta = 0.72$ isosurface) belonging to SSD-III, (c) point at $s = 12.15 \text{ amu}^{1/2} \text{ bohr}$ ($\eta = 0.86$ isosurface, alpha electrons) belonging to SSD-IV, (d) point at $s = 12.15 \text{ amu}^{1/2} \text{ bohr}$ ($\eta = 0.86$ isosurface, beta electrons) belonging to SSD-IV, (e) DBH-diyl species ($\eta = 0.86$ isosurface, alpha electrons), (f) DBH-diyl species ($\eta = 0.86$ isosurface, beta electrons)

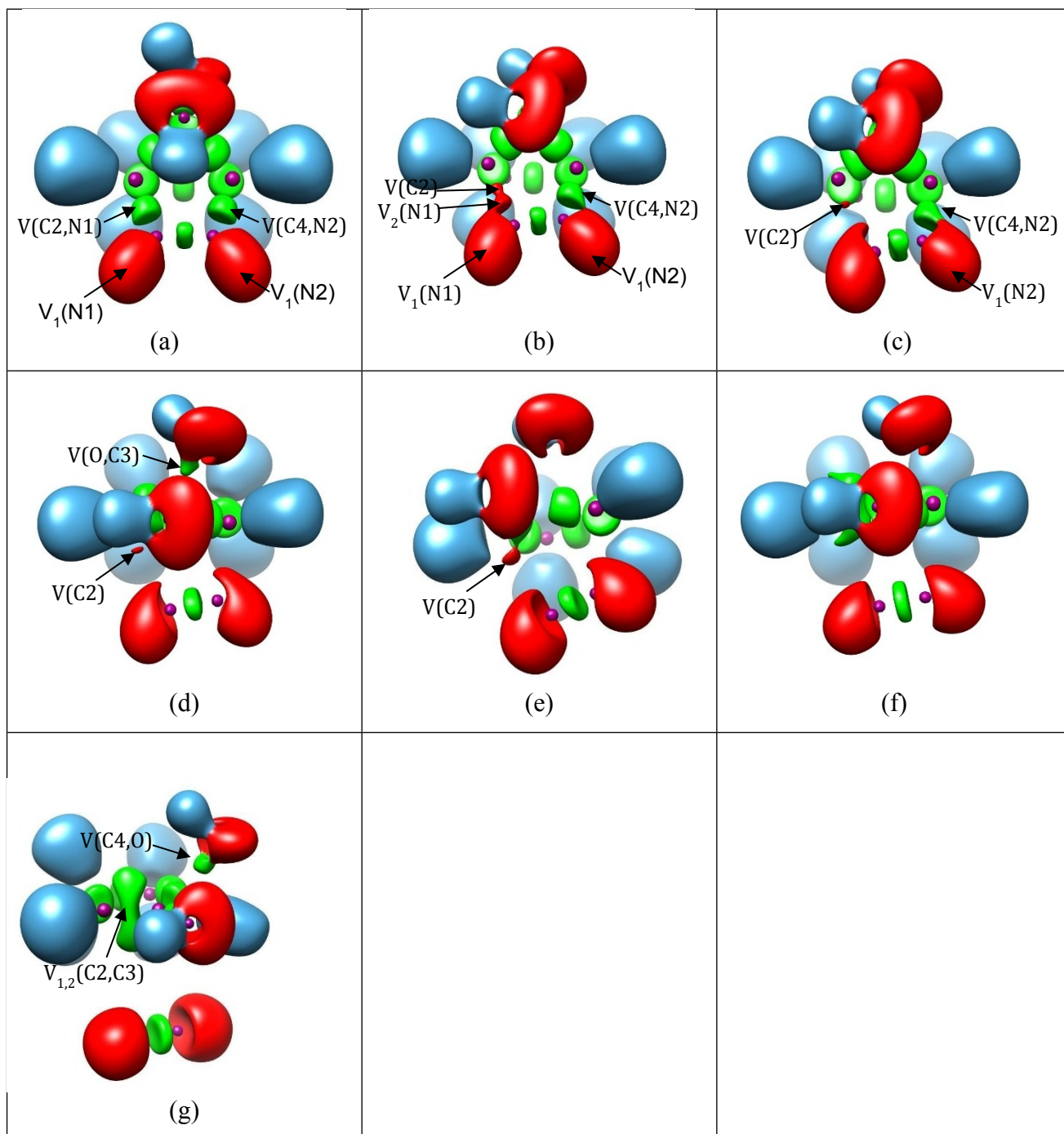


Figure 3S. Snapshots of the ELF localization domains ($\eta = 0.8$ isosurface except where indicated) for selected points along the IRC of the denitrogenation of DBOH *via* the migration pathway: (a) DBOH belonging to the SSD-I domain; (b) point at $s = -4.53$ $\text{amu}^{1/2}$ bohr belonging to SSD-II, (c) point at $s = -2.48$ $\text{amu}^{1/2}$ bohr belonging to SSD-III ($\eta = 0.78$ isosurface); (d) point at $s = -0.88$ $\text{amu}^{1/2}$ bohr belonging to SSD-IV ($\eta = 0.79$ isosurface); (e) TSm-DBOH belonging to SSD-V; (f) point at $s = 1.46$ $\text{amu}^{1/2}$ bohr belonging to SSD-VI; (g) CP-DBOH species (plus N₂) belonging to SSD-VII.

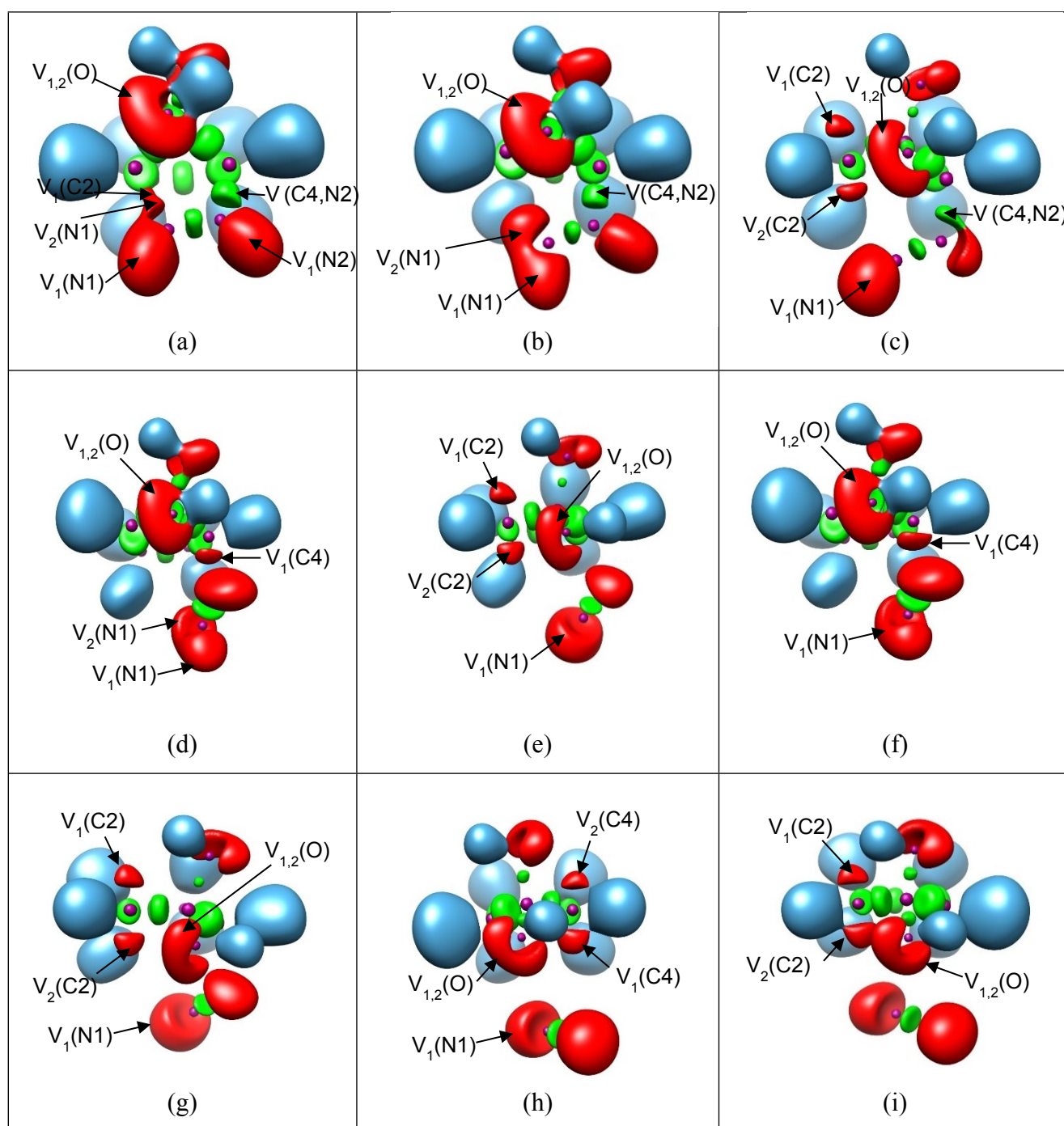


Figure 4S. Snapshots of the ELF localization domains ($\eta=0.8$ isosurface except where indicated) for selected points along the IRC of the DBOH denitrogenation process *via* the *stepwise* reaction pathway (see DBOH belonging to SSD-I in Figure 3Sa). (a) Point belonging to SSD-II; (b) TSS1 belonging to SSD-III (alpha electrons); (c) TSS1 belonging to SSD-III ($\eta=0.857$ isosurface beta electrons). (d) point belonging to SSD-IV (alpha electrons); (e) point belonging to SSD-IV ($\eta=0.857$ isosurface, beta electrons); (f) point belonging to SSD-V (alpha electrons); (g) point belonging to SSD-V ($\eta=0.857$ isosurface, beta electrons); (h) DBOH-diyl species plus N_2 , belonging to SSD-VI ($\eta=0.84$ isosurface, alpha electrons); (i) DBOH-diyl species plus N_2 , belonging to SSD-VI ($\eta=0.84$ isosurface, beta electrons).

Cartesian coordinates:

a) DBH (optimized at B3LYP/6-311+G(2d,p) level)

C	-0.000043	0.000436	-0.000102
C	-0.000004	-0.000306	1.554759
C	2.146904	0.000341	1.104290
C	1.521891	0.000620	-0.319393
H	-0.520247	-0.871482	-0.395548
H	-0.500091	0.893436	-0.377380
H	1.839567	-0.870998	-0.890875
H	1.827803	0.893900	-0.865569
C	1.189776	0.904889	1.885359
H	1.413442	0.954745	2.951702
H	1.102760	1.909897	1.472038
N	0.560599	-1.348267	1.909199
N	1.777068	-1.347793	1.654318
H	-0.958432	0.168778	2.036566
H	3.218058	0.170110	1.160160

b) DBOH (optimized at M05-2X/6-311+G(2d,p) level)

C	0.005411	0.005918	0.009264
C	0.009365	0.008131	1.554275
C	2.156603	0.007005	1.090776
C	1.523021	0.005941	-0.316998
H	-0.509078	-0.873317	-0.366228
H	-0.485192	0.898047	-0.366277
H	1.837875	-0.869718	-0.876011
H	1.811659	0.900305	-0.860476
C	1.197864	0.925471	1.856464
N	0.575712	-1.309697	1.914679
N	1.784852	-1.311182	1.654028
H	-0.934857	0.203886	2.048206
H	3.220258	0.196339	1.162318
O	1.582707	1.025852	3.192476
H	0.844542	1.376025	3.701028
O	0.991086	2.193028	1.301570
H	1.747149	2.738450	1.542920

Mathematical model

Originally, the ELF function has been designed to measure the Fermi hole curvature calculated at the Hartree–Fock level. Savin’s interpretation in terms of local excess kinetic energy due to Pauli repulsion [1] gave support to the calculation of ELF from Kohn–Sham orbitals. ELF has been alternatively interpreted, in terms of localized orbitals [2] and as the nonadditive (interorbital) Fisher information contained in the electron distribution [3]. Subsequently, a generalization of Dobson’s interpretation has been achieved independently by Kohout et al. [4] and by Silvi [5] who introduced a more general localization function, namely the spin pair composition defined as:[6]

$$c_{\pi} = \bar{N}(r)^{-\frac{8}{3}} \bar{N}_{||}(r)$$

in which $\bar{N}(r)$ denotes the number of same spin pair within a sampling volume centered at \mathbf{r} containing $\bar{N}(r)$ electrons, i.e.,

$$\begin{aligned} \bar{N}_{||}(r) &= \iint_{v(r)} (\pi^{\alpha\alpha}(r_1, r_2) + \pi^{\beta\beta}(r_1, r_2)) dr_1 dr_2 \bar{N}(r) \\ &= \int_{v(r)} \rho(r) dr \end{aligned}$$

where $\pi^{\sigma\sigma}(r_1, r_2)$ and $\rho(r)$, respectively, denote the $\sigma\sigma$ pair function and the electron density distribution. The spin pair composition c_{π} function is calculated at different points presenting a maximum value at the center of the box. It has been shown that ELF is an excellent approximation of the spin pair composition [5] enabling its generalization to correlated wave functions [7]. In practice, the localization function adopts a lorentzian $n(r) = (1 + c_{\pi}^2(r))^{-1}$ form which confines its values in the [1, 0] interval.

[1] Savin A, Jepsen O, Flad J, Andersen OK, Preuss H, Vonschnering HG, *Angew. Chem. Int. Ed.* **1992**, *31*, 187

[2] Burdett JK, McCormick TA *J Phys Chem A*, **1998**, *102*, 6366

[3] Nalewajski RF, Koster AM, Escalante S J, *Phys Chem A*, **2005**, *109*, 10038

[4] Kohout M, Wagner ER, Grin Y, *Int J Quantum Chem*, **2006**, *106*, 1499

[5] Silvi B, *J Phys Chem A*, **2003**, *107*, 3081

[6] This correlated version, derived from the analysis of the pair functions has been implemented in the ToPMoD package

[7] Matito E, Silvi B, Duran M, Sola M, *J Chem Phys*, **2006**, *125*, 024301